Available online at www.sciencedirect.com
SCIENCE DIRECT
ELSEVIER
Journal of Physics and Chemistry of Solids 67 (2006) 1469–1476
JOURNAL OF PHYSICS AND CHEMISTRY OF SOLIDS
www.elsevier.com/locate/jpcs

Preparation and thermal decomposition studies of L-tyrosine intercalated MgAl, NiAl and ZnAl layered double hydroxides

Min Wei*, Xiangyu Xu, Jing He, Qi Yuan, Guoying Rao, David G. Evans, Min Pu, Lan Yang

State Key Laboratory of Chemical Resource Engineering, Beijing University of Chemical Technology, Beijing 100029, PR China

Received 1 November 2005; received in revised form 25 January 2006; accepted 27 January 2006

Abstract

L-Tyrosine (represented as L-Tyr) intercalated MgAl, NiAl and ZnAl layered double hydroxides (LDHs) have been obtained by the method of coprecipitation. In situ FT-IR, in situ HT-XRD and TG-DTA measurements allow a detailed understanding of the thermal decomposition process for the three intercalated composites. In situ HT-XRD reveals that the layered structure of L-Tyr/MgAl-LDH collapses completely at 450 °C with the first appearance of reflections of a cubic MgO phase, while the corresponding temperature for L-Tyr/NiAl-LDH is some 50 °C lower. In contrast, there is a major structural change in L-Tyr/ZnAl-LDH at 250 °C as shown by the disappearance of its (0 0 6) and (0 0 9) reflections at this temperature accompanied by the appearance of reflections of ZnO. In situ FT-IR experiments give information about the decomposition of the interlayer -Tyr ions. The decomposition temperature of L-Tyr in the ZnAl host is about 50 °C lower than the corresponding values for the MgAl and NiAl hosts. TG-DTA curves show a significant weight loss step (170–260 °C) in L-Tyr/ZnAl-LDH which is due to the dehydroxylation of the host layers, with a corresponding weak endothermic peak at 252 °C. This temperature range is much lower than that observed for MgAl and NiAl hosts, indicating that the ZnAl-LDH layers are relatively unstable. The data indicate that the order of thermal stability of the three intercalates is: L-Tyr/MgAl-LDH > L-Tyr/NiAl-LDH > L-Tyr/ZnAl-LDH.
© 2006 Elsevier Ltd. All rights reserved.

Keywords: A. Inorganic compounds; C. Infrared spectroscopy; C. X-ray diffraction; D. Phase transitions

1. Introduction

Layered double hydroxides (LDHs), which are widely known host–guest materials, have received considerable attention due to their ability to intercalate a wide variety of anions. LDHs can be represented by the general formula $\left[M^{II}_{1-x}M^{III}_{x}(OH)_2\right]^{x+}(A^{n-})_{x/n}\cdot mH_2O$ [1], where M^{II} and M^{III} are di- and tri-valent metal cations, respectively; A^{n-} is an exchangeable inorganic or organic anion and the parameter x which determines the charge density of the layers, is equal to the molar ratio $M^{III}/(M^{II}+M^{III})$. LDHs consist of positively charged metal hydroxide layers, between which the anions (along with water) are intercalated in order to compensate the positive layer charges. Various inorganic or organic anions have been introduced between the hydroxide layers by simple ion-exchange reactions or coprecipitation. LDHs are now well established as excellent anion-exchange materials and their extensive intercalation chemistry has widespread applications in areas such as heterogeneous catalysis [2,3], optical materials [4,5], biomimetic catalysis [6,7], separation science [8,9], DNA reservoirs [10] and medical science [11,12].

Recently, considerable attention has been paid to the intercalation of biomolecules or pharmaceutical agents into LDHs. The intercalation of amino acids [13,14], nucleoside monophosphates and deoxyribonucleic acid [15], c-antisense oligonucleotides (As-myc) [16], nucleoside monophosphates and deoxyribonucleic acid (DNA) and vitamin (A,C,E) into LDHs have been reported [16,17]. The biomolecule intercalated LDHs hybrids have potential usage as novel reservoirs and carriers.

The thermal stability of the intercalated biomolecules has rarely been investigated, however, although it is a very important aspect which should be considered when using

*Corresponding author. Tel.: +86 10 64412131; fax: +86 10 64425385.
E-mail address: weimin@mail.buct.edu.cn (M. Wei).

0022-3697/$ - see front matter © 2006 Elsevier Ltd. All rights reserved.
doi:10.1016/j.jpcs.2006.01.118

LDHs-biomolecules as reservoirs or carriers. We have studied the thermal decomposition of L-aspartic acid intercalated LDHs by in situ techniques [18], and found that the thermolysis of this hybrid material is quite different from that of the pristine L-aspartic acid.

Generally, ex situ X-ray diffraction (XRD) and thermal analysis have been used to investigate the decomposition process of LDHs. Ex situ studies have the disadvantage that mixed oxides derived from LDHs may rehydrate and reconstruct to the original structure at ambient temperature in air [19]. Hou et al. reported the use of relative humidity controlled powder XRD data which provide greatly increased understanding of the effects of hydration state on the structure and dynamical behavior of interlayer and surface anions and the factors controlling the expansion behavior of this group of minerals [20]. In situ infrared spectroscopy has been employed to provide structural information about the dehydroxylation and decarbonation processes [21,22]. High-temperature XRD (HT-XRD) has been used as an in situ technique to investigate the decomposition and reconstruction mechanism of Mg–Al–CO_3 LDH [23], since thermally metastable phases which are not apparent in conventional XRD measurements can be observed by the in situ HT-XRD technique.

In our former work, L-tyrosine has been intercalated into MgAl, ZnAl and NiAl LDHs by coprecipitation. It is found that intercalation can inhibit racemization of L-tyrosine under the influence of sunlight, high temperature or ultraviolet light [24]. In the present study, in situ FT-IR, in situ HT-XRD and TG-DTA measurements were used to characterize the thermolysis process for the three intercalated composites. Other workers have found that the type of host layer has a very important influence on the thermal decomposition process in LDHs [22,25], and this work provides a detailed understanding of the differences in thermal properties of MgAl, ZnAl and NiAl LDHs intercalated with the same guest.

2. Experimental Section

2.1. Preparation of L-Tyr intercalated MgAl, ZnAl and NiAl LDHs

L-Tyr intercalated MgAl, ZnAl and NiAl LDHs were prepared according to our former work [24]. The chemical compositions of the three materials are: $Mg_{4.08}Al_{2.00}(OH)_{12.18}(C_9H_{10}NO_3)_{1.16}(NO_3)_{0.82} \cdot 4.62H_2O$, $Zn_{3.92}Al_{2.00}(OH)_{11.84}(C_9H_{10}NO_3)_{1.42}(NO_3)_{0.58} \cdot 4.48H_2O$ and $Ni_{4.00}Al_{2.00}(OH)_{12.00}(C_9H_{10}NO_3)_{1.56}(NO_3)_{0.44} \cdot 4.56H_2O$.

2.2. Characterization

The in situ powder XRD measurements were performed on a Rigaku D/MAX2500VB2+/PC diffractometer in the temperature range 25–700 °C under vacuum conditions, using CuKα radiation ($\lambda = 0.154$ nm) at 40 kV, 20 mA, with step scans of 5 °/min, and a 2θ angle ranging from 2 ° to 70 °. The rate of temperature increase was 10 °C/min with a holding time of 5 min before each measurement.

The in situ Fourier transform infrared spectra were recorded using a Nicolet 605XB FT-IR spectrometer in the range 4000–400 cm^{-1} with 4 cm^{-1} resolution under flowing N_2 (65 mL/min) with a heating rate of 5 °C/min in the range 25–450 °C. The standard KBr disk method (1 mg of sample in 100 mg of KBr) was used.

Thermogravimetric analysis and differential thermal analysis (TG–DTA) were measured on a PCT-1A thermal analysis system with a heating rate of 5 °C/min under air.

Microanalysis of metals was performed by inductively coupled plasma (ICP) emission spectroscopy on a Shimadzu ICPS-7500 instrument using solutions prepared by dissolving the samples in dilute HNO_3. Carbon, hydrogen and nitrogen analyses were carried out using an Elementarvario elemental analysis instrument.

3. Results and discussion

3.1. Structure of L-Tyr intercalated MgAl, NiAl and ZnAl LDHs

Fig. 1 shows the powder XRD patterns of the L-Tyr intercalated MgAl-, NiAl- and ZnAl-LDHs. In each case, the reflections can be indexed to a hexagonal lattice with *R*-3 m rhombohedral symmetry, commonly used for the description of LDH structure [26]. However, as is often the case, several of the (*h k l*) reflections disappear or broaden. The values of basal spacing of the intercalates are 1.69, 1.71 and 1.72 nm, respectively, for the three different host layers, which are close to that previously reported by Fudala et al. for a Zn_3Al L-Tyr/LDH (1.75 nm) [14]. It should be noted that some amount of nitrate was cointercalated between the host layers by elemental

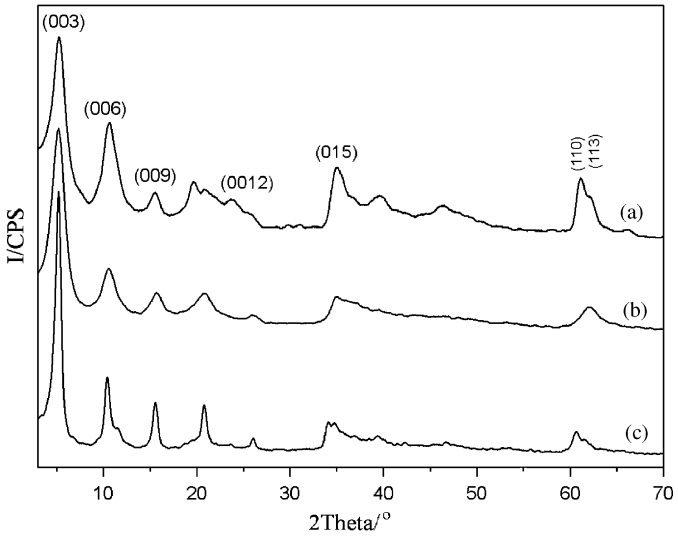

Fig. 1. Powder XRD patterns of (a) L-Tyr/MgAl-LDH, (b) L-Tyr/NiAl-LDH and (c) L-Tyr/ZnAl-LDH.

analysis in our previous work [24], which may be related to the reason that the large L-Tyr anions alone cannot maintain the charge balance between host and guest. Fudala et al. have also confirmed the cointercalation of nitrate in the preparation of amino acid-LDH composites [14]. In addition, the peak around 19.8° 2θ in Fig. 1a (L-Tyr/MgAl-LDH) is attributed to the (0 0 6) reflection of a separate NO_3^- LDH phase, while the peak around 10.5° 2θ may be a superposition of the (0 0 6) reflection of L-Tyr/MgAl-LDH and the (0 0 3) reflection of NO_3^- LDH, accounting for its broadening. This will be further discussed in the section of in situ HT-XRD. Moreover, the shoulder at 11.5° 2θ in Fig. 1c (L-Tyr/ZnAl-LDH) was observed. This is possibly due to the presence of small amount of a CO_3^{2-} LDH impurity phase, which is hardly avoided even when intercalation reactions are carried out under nitrogen. Newman et al. gave a detailed analysis of the arrangement of two amino acid guest species (phenylalanine and tyrosine) in LDH interlayers using molecular dynamics calculations, and concluded that the guests interact with the LDH host layers through a hydrogen bonding network [27]. If the thickness of the LDH layer (0.48 nm) is subtracted from the basal spacing [28], the values of gallery height of MgAl-, NiAl- and ZnAl-LDH are calculated to be 1.21, 1.23 and 1.24 nm, respectively, which are longer than the length of the L-Tyr anion (0.86 nm, calculated using Chemwindow 6.0). This suggests that L-Tyr anions are accommodated in the interlayer region as an interdigitated bilayer arrangement, with the phenyl groups in the center of the interlayer galleries and the closest contact with the layers made through the oxygen atoms of the carboxylate group. Nitrate anions and water molecules are cointercalated in the gallery, participating in the formation of hydrogen bonding between the L-Tyr anions and the host layers. A similar structure is expected for our three materials.

3.2. Thermolysis of L-Tyr intercalated MgAl, NiAl and ZnAl LDHs

3.2.1. Thermolysis of L-Tyr/LDHs studied by in situ HT-XRD

The in situ variable temperature powder XRD patterns of L-Tyr/MgAl-LDH, L-Tyr/NiAl-LDH and L-Tyr/ZnAl-LDH in the range 20–700 °C are shown in Fig. 2A, B and C, respectively. The variation in the d_{003} basal spacing of the three intercalated products with temperature is shown in Fig. 3.

It can be observed in Fig. 2 that the (0 0 3), (0 0 6) and (0 0 9) diffraction peaks of all three L-Tyr intercalated LDHs move to higher angle 2θ with increasing temperature, indicating a decrease in basal spacing. The value of d_{003} decreases in distinct two steps as shown in Fig. 3. The first, from 20 to 150 °C, is related to two possible reasons: (1) the loss of the hydrogen bonding space as a result of deintercalation of interlayer water molecules [27] and (2) the reorientation of the interlayer guest anions [28]. The

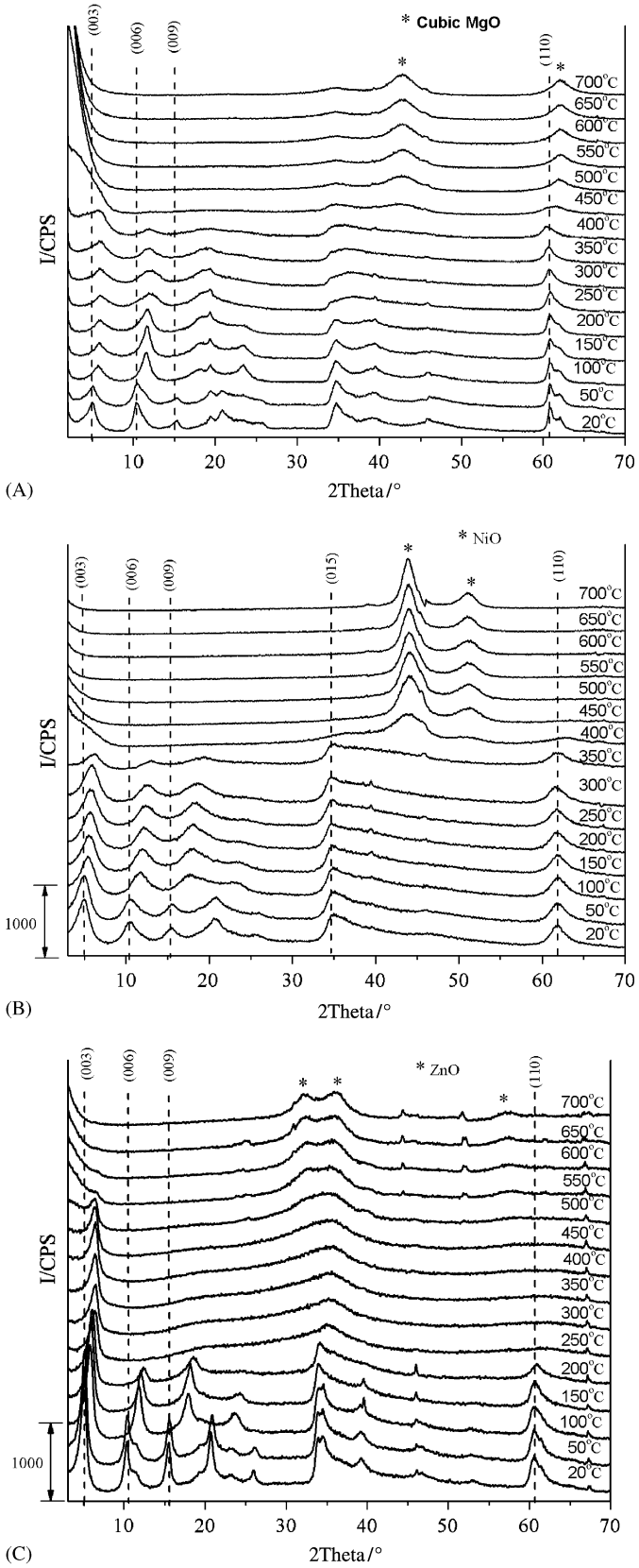

Fig. 2. In situ XRD patterns for the thermal decomposition of (A) L-Tyr/MgAl-LDH, (B) L-Tyr/NiAl-LDH, (C) L-Tyr/ZnAl-LDH in the temperature range 20–700 °C.

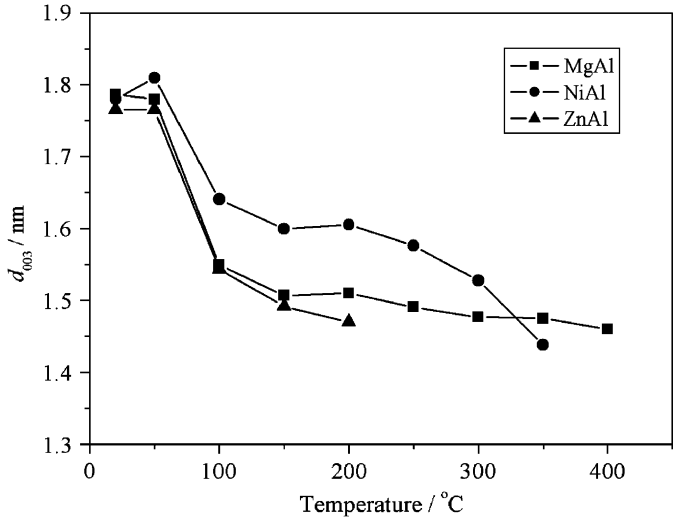

Fig. 3. Variation in d_{003} basal spacing of L-Tyr intercalated LDHs with temperature.

observed decreases in d_{003} values for L-Tyr/MgAl-LDH, L-Tyr/NiAl-LDH and L-Tyr/ZnAl-LDH are 0.28, 0.19 and 0.27 nm, respectively, providing evidence in support of the structural model of L-Tyr/LDH discussed above. A further decrease in the value of d_{003} is observed in the temperature range 150–400, 150–350 and 150–200 °C, for the sample of L-Tyr/MgAl-LDH, L-Tyr/NiAl-LDH and L-Tyr/ZnAl-LDH, respectively. This contraction is attributed not only to the decomposition of the intercalated L-Tyr anions and the cointercalated nitrate, but also to the dehydroxylation of the host layers because the reflections declined and broadened continuously upon increasing temperature (Fig. 2). The difference in the temperature scope corresponds to the different thermal stability of the three samples. This will be further discussed in the next section.

As shown in Fig. 2A, the intensities of the (0 0 3), (0 0 6) and (0 0 9) reflections of L-Tyr/MgAl-LDH decrease gradually with increasing temperature, and the layered structure collapses completely at 450 °C with the first appearance of reflections from a cubic MgO phase at about 34.6°, 42.8° and 62.5° [29]. Crystallization of MgO occurs at 450 °C, over 50 °C higher than that usually observed during the calcination of Mg–Al–CO_3 LDH [23,30]. The reflections of MgO become stronger as the temperature increases from 500 to 700 °C. For the impurity NO_3^- LDH phase, its (0 0 6) peak at 19.8° 2θ became weaker along with the increase of temperature, and almost disappeared at 300 °C. For L-Tyr/NiAl-LDH (Fig. 2B), the temperature at which the reflections corresponding to the LDH phase disappear and those of cubic NiO appear is 400 °C [31], some 50 °C lower than that for L-Tyr/MgAl-LDH. The L-Tyr/ZnAl-LDH behaves differently from the other two samples however (Fig. 2C). The reflections of the LDH phase become weaker with increasing temperature, and the (0 0 6) and (0 0 9) reflections disappear at 250 °C accompanying the appearance of reflections of hexagonal ZnO [32]. The (0 0 3) peak of the LDH continues to become weaker while the reflections of ZnO become stronger with further increase of temperature between 250 and 500 °C, indicating the coexistence of the two phases. The XRD data reveal that there is a major structural change in the L-Tyr/ZnAl-LDH at 250 °C, yet a small fraction of layered structure is still present at 500 °C. When the temperature increases to 550 °C, the (0 0 3) reflection of the LDH cannot be observed and only ZnO remains. The diffraction peaks of ZnO gradually become stronger in the temperature range 550–700 °C. Our results indicate that the thermal stability of the three intercalates varies in the order: MgAl > NiAl > ZnAl. This might be due to the reason that the transformation of hexagonal ZnAl-LDH to hexagonal ZnO is much easier than that of hexagonal MgAl-LDH (or NiAl-LDH) to cubic MgO (or NiO).

3.2.2. Thermolysis of L-Tyr/LDHs studied by in situ FT-IR

3.2.2.1. In situ FT-IR spectra of L-Tyr/MgAl-LDH. In order to investigate the thermal decomposition of L-Tyr intercalated LDH, in situ FT-IR was used to record the infrared spectra during the decomposition process. Fig. 4 displays the spectra of L-Tyr/MgAl-LDH in the temperature range 25–450 °C. In the room temperature spectrum, the broad band centered at 3458 cm^{-1} corresponds to the O–H stretching vibration of surface and interlayer water molecules [33], which are found at lower frequency in LDHs compared with the O–H stretch in free water at

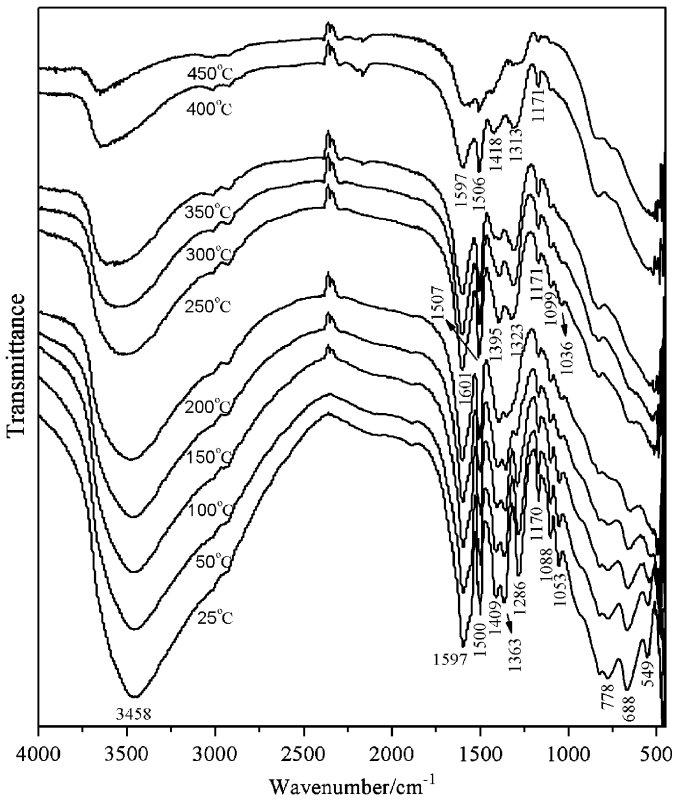

Fig. 4. In situ FT-IR spectra for the thermal decomposition of L-Tyr/MgAl-LDH.

3600 cm^{-1} [34]. This is attributed to the formation of hydrogen bonding of interlayer water with the different guest anions as well as with the hydroxide groups of the layers. The positions and relative intensities of the bands at 1597, 1500, 1409 and 1286 cm^{-1}, closely resemble those in the spectrum of pristine L-Tyr and in that of Zn_3Al L-Tyr/LDH [14]. The other absorption bands below 1000 cm^{-1} are generally assigned to the metal-oxygen skeletal stretching and bending vibrations of the LDH sheets [35]. The bands centered at 778 and 688 cm^{-1} are attributed to M–O (M–O–M or O–M–O) bending deformation vibrations and M–O–H stretching vibrations in the brucite-like sheets, respectively [34].

The O–H stretching vibration becomes weaker with a slight shift to high frequency on increasing the temperature, although it is still present at 450 °C, indicative of the loss of water molecules as well as the dehydroxylation of the LDH layers. At 25 °C, the asymmetric and symmetric stretching vibrations of the carboxylate groups are observed at 1597 and 1409 cm^{-1}, respectively, and on raising the temperature to 150 °C the difference, $\Delta v(\Delta v = v_{as} - v_s)$, between their position increases from 188 to 201 cm^{-1}. According to Nakamoto [34], the value of Δv gives information about the symmetry of the interaction between the carboxylate groups and the hydroxylated layers. Therefore, it may indicate there is some change in the interaction between the guest and host associated with the loss of hydrogen bonding space as a result of liberation of interlayer water. This is in agreement with the in situ HT-XRD measurements which show that there is a contraction in the value of d_{003} in this temperature range. No significant changes in the positions of the four absorption bands of L-Tyr are observed between room temperature and 200 °C, indicating that the intercalated guest is stable in this temperature range. However, obvious changes in band intensity are observed at about 250 °C. The four characteristic bands of L-Tyr become weaker and the value of Δv shows a further increase. Moreover, they become rather weak when the temperature increases to 450 °C. This implies that the decomposition of intercalated L-Tyr begins at about 250 °C, and these bands become even weaker at 450 °C, corresponding to further decomposition of L-Tyr. The band at 666 cm^{-1} assigned to the M–O–H stretching vibrations in the brucite-like sheets becomes weaker on increasing the temperature, and disappears above 350 °C, suggesting that dehydroxylation of the host layers occurs.

3.2.2.2. In situ FT-IR spectra of L-Tyr/ZnAl-LDH. Fig. 5 shows the FT-IR spectra of L-Tyr/ZnAl-LDH in the temperature range 25–450 °C. The broad band corresponding to the O–H stretching vibration of surface and interlayer water molecules at room temperature is centered at 3433, 26 cm^{-1} lower than that in L-Tyr/MgAl-LDH, indicative of a stronger hydrogen bonding interaction. This band becomes weaker with a slight shift to high frequency on increasing the temperature, and almost disappears at

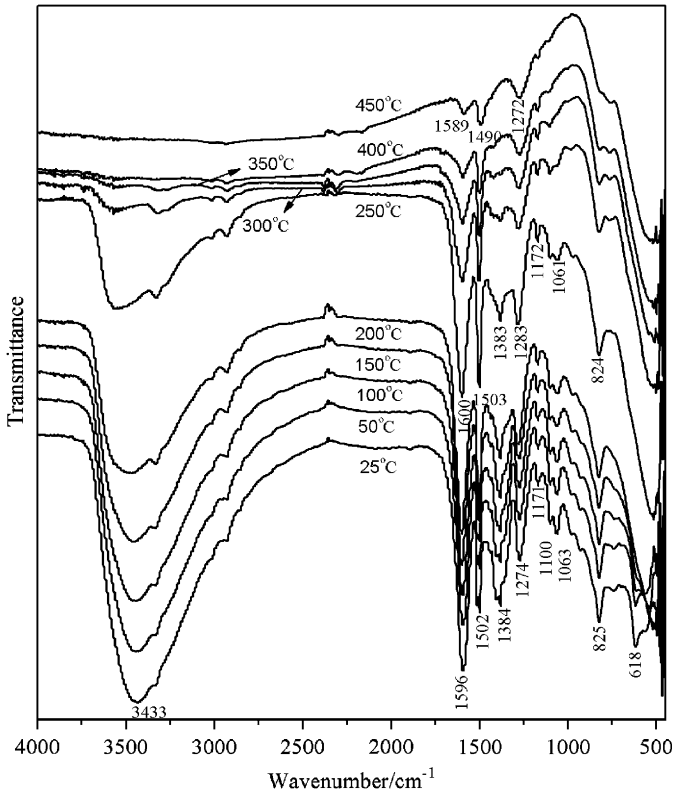

Fig. 5. In situ FT-IR spectra for the thermal decomposition of L-Tyr/ZnAl-LDH.

about 350 °C, indicating the loss of water molecules as well as the dehydroxylation of the LDH layers. Comparison with the same band in L-Tyr/MgAl-LDH which is still present at 450 °C reveals that the ZnAl layered structure is less stable than the MgAl host layers, which has been confirmed by in situ HT-XRD in that the (0 0 6) and (0 0 9) reflections of L-Tyr/ZnAl-LDH disappear at 250 °C. At room temperature, the characteristic absorption bands of the L-Tyr anion are observed at 1596, 1502, 1384 and 1274 cm^{-1}. Their intensities become weaker in the temperature range 20–150 °C, and there is a significant decrease in intensity at 200 °C. The intensities of these bands decrease markedly between 200 and 350 °C, and the band originally at 1384 cm^{-1} eventually disappears completely at 400 °C. The above results imply that the decomposition of intercalated L-Tyr begins at about 200 °C, and there is a major structural change at 400 °C. The decomposition temperature of L-Tyr in the ZnAl host is lower by about 50 °C than that in the MgAl host lattice. Furthermore, the band at 618 cm^{-1} attributed to the M–O–H stretching vibrations disappears at 200 °C, indicating the instability of the layered structure of the ZnAl host.

3.2.2.3. In situ FT-IR spectra of L-Tyr/NiAl-LDH. Infrared spectra recorded at room temperature, as well as during the decomposition of the L-Tyr/NiAl-LDH in the temperature range 25–450 °C are presented in Fig. 6. Compared with L-Tyr intercalated MgAl and ZnAl LDHs,

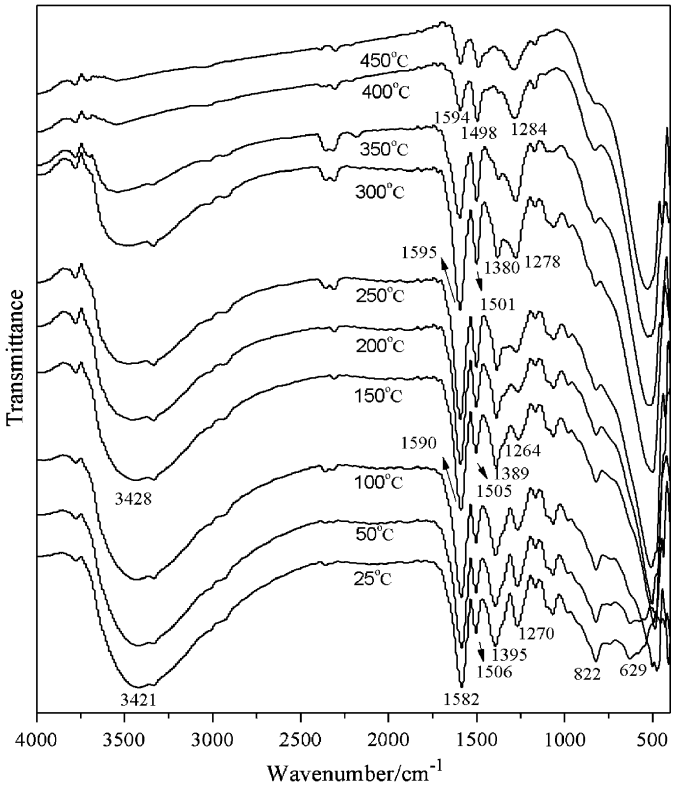

Fig. 6. In situ FT-IR spectra for the thermal decomposition of L-Tyr/NiAl-LDH.

the O–H stretching vibration at room temperature is observed at much lower frequency, 3421 cm^{-1}, indicating the strongest interlayer hydrogen bonding of the three LDH intercalates occurs for the NiAl LDH host. As for L-Tyr intercalated MgAl and ZnAl LDHs, this band becomes weaker with a slight shift to high frequency on increasing the temperature, and almost disappears at about 450 °C. This temperature is higher than the corresponding value for the ZnAl host layers, but lower than that for the MgAl host lattice, which suggests that the thermal stability of NiAl LDH is lower than that of MgAl but higher than that of ZnAl LDH. This is in accordance with the results of in situ HT-XRD. The four absorption bands of L-Tyr are located at 1582, 1506, 1395 and 1270 cm^{-1}. No significant changes in the positions of these bands occur between 25 and 200 °C, but marked changes are observed at about 250 °C. The four characteristic bands of L-Tyr become much weaker and the value of $\Delta\nu$ shows an increase (from 187 cm^{-1} at room temperature to 212 cm^{-1} at 250 °C). Eventually, the band originally at 1395 cm^{-1} disappears completely at 400 °C. This indicates that the decomposition of intercalated L-Tyr begins at about 250 °C, and a marked structural change is observed at 400 °C. These bands become even weaker at 450 °C, corresponding to further decomposition of L-Tyr. Moreover, the band at 629 cm^{-1} attributed to the M–O–H stretching vibrations cannot be observed at 200 °C, indicating that the layered structure of the NiAl host lattice is less stable than that of the MgAl host (whose bands disappear at 350 °C).

It should be noted that the stretching absorption of cointercalated nitrate (normally around 1385 cm^{-1}) was superposed by the characteristic absorption bands of L-Tyr in the three composites, as a result the accurate information on the NO_3^- decomposition cannot obtained.

3.2.3. TG and DTA of L-Tyr/LDHs

The TG and DTA curves of L-Tyr/MgAl-LDH, L-Tyr/NiAl-LDH and L-Tyr/ZnAl-LDH are shown in Figs. 7 and 8, respectively. The thermal decomposition of L-Tyr/MgAl-LDH is characterized by three weight loss steps (Fig. 7a): the first one from room temperature to 150 °C corresponds to the removal of surface adsorbed water (below about 100 °C) and interlayer water molecules resulting in the decrease in interlayer spacing observed in Fig. 3; the second one (250–400 °C), involving a gradual weight loss, is a result of the decomposition of L-Tyr anions and cointercalated nitrate, and dehydroxylation of the brucite-like layers, which is consistent with the results of in situ HT-XRD and in situ FT-IR; the third one with a sharp weight loss in the temperature region 400–490 °C with a corresponding exothermic maximum at 452 °C in the DTA curve (Fig. 8a) is due to the combustion of the carbonaceous residue.

As shown in Fig. 7b, there are also three weight loss steps during the thermal decomposition of L-Tyr/NiAl-LDH. The origin of first one (20–150 °C) is the same as that for L-Tyr/MgAl-LDH, i.e., the removal of surface and interlayer water; the second one between 200 and 340 °C is due to the decomposition of L-Tyr ions, dehydroxylation of the brucite-like layers, and the decomposition of nitrate, which occurs about 50 °C lower than the corresponding process for L-Tyr/MgAl-LDH. This is in accordance with the results obtained by in situ HT-XRD in that the complete collapse of the layered structure of L-Tyr intercalated NiAl LDH occurs some 50 °C lower than that for MgAl LDH. The third weight loss step (340–380 °C)

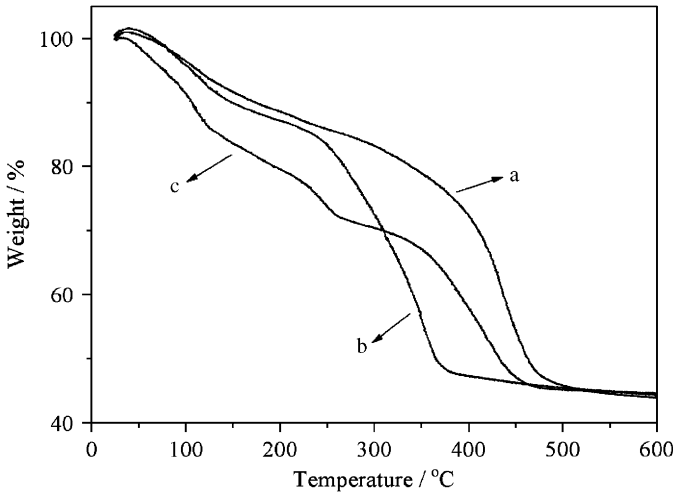

Fig. 7. TG curves for (a) L-Tyr/MgAl-LDH, (b) L-Tyr/NiAl-LDH and (c) L-Tyr/ZnAl-LDH.

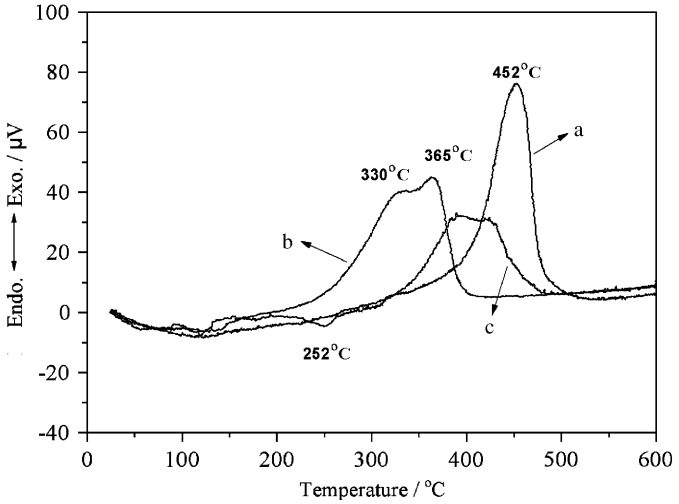

Fig. 8. DTA curves for (a) L-Tyr/MgAl-LDH, (b) L-Tyr/NiAl-LDH and (c) L-Tyr/ZnAl-LDH.

corresponds to the dehydroxylation of the brucite-like layers and combustion of the decomposed materials. It can be observed in the DTA curve (Fig. 8b) that there are two overlapping exothermic peaks at 330 and 365 °C related to the combustion of the interlayer carbonaceous residue.

The TG and DTA curves of L-Tyr/ZnAl-LDH show considerable differences from the other two intercalates. The thermal decomposition of L-Tyr/ZnAl-LDH involves four steps (Fig. 7c): the first one (20–130 °C) is the result of the removal of surface and interlayer water; the second one in the temperature range 170–260 °C can be assigned to the dehydroxylation of the host layers, with a corresponding weak endothermic peak at 252 °C in the DTA curve (Fig. 8c). This is in accordance with the results obtained by in situ HT-XRD in that the intensities of the (0 0 6) and (0 0 9) reflections of L-Tyr/ZnAl-LDH decrease significantly at 200 °C and disappear at 250 °C accompanying the appearance of reflections of ZnO, indicating there is a structural transformation at 250 °C. The third weight loss step (260–390 °C) is attributed to the decomposition of L-Tyr ions and dehydroxylation of the brucite-like layers; the last one (390–450 °C) corresponds to the combustion of the carbonaceous residue, with exothermic peaks (at 390 and 425 °C) in the DTA curve (Fig. 8c). Compared with L-Tyr/MgAl-LDH and L-Tyr/NiAl-LDH, the dehydroxylation temperature of the L-Tyr/ZnAl-LDH is lower, indicating the instability of the ZnAl host layers. However, the combustion of the interlayer organic materials in the ZnAl host occurs at temperature between those for NiAl and MgAl hosts, which is possibly related to the reason that the combustion reaction is catalyzed by Ni^{2+}.

It can be seen from Fig. 7 that the weight loss of all the three samples was about 55% upon increasing the temperature to 600 °C. On the assumption that only the metal oxides are present at 600 °C, the theoretical weight loss of L-Tyr/MgAl-LDH, L-Tyr/NiAl-LDH and L-Tyr/ZnAl-LDH would be 62.2%, 54.6% and 52.3%, respectively, based on the calculation from their chemical compositions. The comparison between the experimental value and the calculated ones indicates that the Ni–Al and Zn–Al samples existed mainly as metal oxides at 600 °C, while the metal oxides in the Mg–Al sample have not completely formed at this temperature, which is related to its relatively high thermal stability of the host layer. This is in accordance with the temperature order in the appearance of metal oxide obtained by in situ HT-XRD, which has been discussed above (MgO: 450 °C; NiO: 400 °C; ZnO: 250 °C).

4. Conclusions

L-Tyr intercalated MgAl, NiAl and ZnAl LDHs have been obtained by coprecipitation. A combination of techniques, including in situ FT-IR, in situ HT-XRD and TG-DTA measurements allows a detailed understanding of the thermal decomposition process for the three intercalated composites.

In situ HT-XRD reveals the phase transformation of L-Tyr/LDH composites, which includes the destruction of the hydrogen bonding area resulting from the loss of the interlayer water, the decomposition of the intercalated L-Tyr anions and the dehydroxylation of the host layers. For L-Tyr/MgAl-LDH, the layered structure collapses completely at 450 °C, 50 °C higher than that for L-Tyr/NiAl-LDH; while L-Tyr/ZnAl-LDH showed a major structural change at 250 °C, indicative by the disappearance of (0 0 6) and (0 0 9) reflections at this temperature accompanying the appearance of reflections of ZnO. In situ FT-IR has been used to provide structural information about the thermolysis of interlayer L-Tyr as well as the dehydroxylation for the composite LDHs, and TG–DTA data show the weight loss steps and the corresponding thermal properties during the decomposition process, which is in agreement with the results obtained by in situ HT-XRD and in situ FT-IR. Based on the experimental results, it can be concluded that the thermal stability of the host lattice of the three intercalates varies in the order: MgAl > NiAl > ZnAl. Therefore, this work provides an understanding of the thermal stability of hybrids between L-Tyr and LDHs for prospective application as the basis of a novel biomolecule delivery system.

Acknowledgements

This project was supported by the National Natural Science Foundation of China (Project No. 90206004), the Beijing Nova Program (No. 2004A13), the Ministry of Education Science and Technology Research Project of China (Project No. Key 104239) and the Program for Changjiang Scholars and Innovative Research Team in University (PCSIRT).

References

[1] M. Meyn, K. Beneke, G. Lagaly, Inorg. Chem. 29 (1990) 5201.
[2] V.R.L. Constantino, T.J. Pinnavaia, Catal. Lett. 23 (1994) 361.
[3] A. Corma, V. Fornes, F. Rey, A. Cervilla, E. Llopis, A. Ribera, J. Catal. 152 (1995) 237.
[4] M. Ogawa, K. Kuroda, Chem. Rev. 95 (1995) 399.
[5] H. Tagaya, S. Sato, T. Kuwahara, J. Kadokawa, K. Masa, K. Chiba, J. Mater. Chem. 4 (1994) 1907.
[6] B. Sels, D. De Vos, M. Buntinx, F. Pierard, A. Kirsch-De Mesmaeker, P. Jacobs, Nature 400 (1999) 855.
[7] L. Ukrainczyk, M. Chibwe, T.J. Pinnavaia, S.A. Boyd, Environ. Sci. Technol. 29 (1995) 439.
[8] A.M. Fogg, V.M. Green, H.G. Harvey, D. O'Hare, Adv. Mater. 11 (1999) 1466.
[9] A.M. Fogg, J.S. Dunn, S.G. Shyu, D.R. Cary, D. O'Hare, Chem. Mater. 10 (1998) 351.
[10] J.H. Choy, S.Y. Kwak, Y.J. Jeong, J.S. Park, Angew. Chem. Int. Ed. 39 (2000) 4042.
[11] A.I. Khan, L. Lei, A.J. Norquist, D. O'Hare, Chem. Commun. (2001) 2342.
[12] V. Ambrogi, G. Fardella, G. Grandolini, L. Perioli, Int. J. Pharmaceutics 220 (2001) 23.
[13] A. Fudala, I. Palinko, B. Hrivnak, I. Kiricsi, J. Therm. Anal. Calorim. 56 (1999) 317.
[14] A. Fudala, I. Palinko, I. Kiricsi, Inorg. Chem. 38 (1999) 4653.
[15] J. Choy, S. Kwak, J. Park, Y. Jeong, J. Portier, J. Am. Chem. Soc. 121 (1999) 1399.
[16] S.Y. Kwak, Y.J. Jeong, J.S. Park, J.H. Choy, Solid State Ionics 151 (2002) 229.
[17] S.H. Hwang, Y.S. Han, J.H. Choy, Bull. Korean Chem. Soc. 22 (2001) 1019.
[18] Q. Yuan, M. Wei, D.G. Evans, X. Duan, J. Phys. Chem. B 108 (2004) 12381.
[19] J. Pérez-Ramírez, G. Mul, J.A. Moulijn, Vib. Spectrosc. 27 (2001) 75.
[20] X.Q. Hou, D.L. Bish, S.L. Wang, C.T. Johnston, R.J. Kirkpatrick, Am. Mineral. 88 (2003) 167.
[21] J. Pérez-Ramírez, G. Mul, F. Kapteijn, J.A. Moulijn, Appl. Catal. A 204 (2000) 265.
[22] J.T. Kloprogge, R.L. Frost, Phys. Chem. Chem. Phys. 1 (1999) 1641.
[23] E. Kanezaki, Solid State Ionics 106 (1998) 279.
[24] M. Wei, Q. Yuan, D.G. Evans, Z.Q. Wang, X. Duan, J. Mater. Chem. 15 (2005) 1197.
[25] R.L. Frost, W. Martens, Z. Ding, J.T. Kloprogge, J. Therm. Anal. Calorim. 71 (2003) 429.
[26] C. Vaysse, L. Guerlou-Demourgues, C. Delmas, Inorg. Chem. 41 (2002) 6905.
[27] S.P. Newman, T. Di Cristina, V. Coveney, W. Jones, Langmuir 18 (2002) 2933.
[28] V. Prevot, C. Forano, J.P. Besse, F. Abraham, Inorg. Chem. 37 (1998) 4293.
[29] N.G. Schmahl, G.F. Eikerling, Z. Phys. Chem. Neue Folge. (Wiesbaden) 62 (1968) 268.
[30] B. Rebours, E.C. Jean-Baptiste, O. Clause, J. Am. Chem. Soc. 116 (1994) 1707.
[31] N.G. Schmahl, J. Bathel, G.F. Eikerling, Z. Anorg. Allg. Chem. 332 (1964) 230.
[32] O. Garcia-Martinez, Solid State Ionics 63 (1993) 442.
[33] F. Cavani, F. Trifirò, A. Vaccari, Catal. Today 11 (1991) 173.
[34] K. Nakamoto, Infrared and Raman Spectra of Inorganic and Coordination Compounds, fifth ed., Wiley, New York, 1997.
[35] F. Millange, R.I. Walton, L.X. Lei, D. O'Hare, Chem. Mater. 12 (2000) 1990.